Angular Distribution of Cu^{64} Nuclei from the $Cu^{65}(He^3,\alpha)$ Reaction*

N. T. PORILE AND I. FUJIWARA†
Department of Chemistry, Purdue University, Lafayette, Indiana

AND

R. L. HAHN
Oak Ridge National Laboratory, Oak Ridge, Tennessee

(Received 4 December 1967)

The angular distribution of Cu^{64} nuclei produced in the interaction of He^3 ions with Cu^{65} has been measured over the energy range 12–32 MeV. The results have been compared with a distorted-wave calculation for the (He^3,α) pickup process and with a statistical-theory calculation for the evaporation process. It is found that contributions from both mechanisms are required to reproduce the data. The compound-nuclear process, which involves the evaporation of an α particle at the lower energies and of four nucleons at the higher ones, accounts for most of the Cu^{64} yield at small angles to the beam, whereas the pickup process accounts for most of it at large angles.

I. INTRODUCTION

THE measurement of the average projected ranges of recoil products formed in intermediate-energy nuclear reactions can be used to derive information about the linear momentum transferred by the projectile to the target nucleus. The momentum values obtained in this fashion may be compared with those expected on the basis of compound-nucleus formation in order to determine if this is the principal reaction mechanism.

Measurements and comparisons of this type have recently been reported for various reactions of Cu^{65} with He^4 and He^3 ions.[1,2] It was found that the (α, xn) (x=1–3) and $(He^3, 2n)$ reactions led to recoil ranges that were in good agreement with the values expected on the basis of compound-nucleus formation. On the other hand, the ranges of the (He^3,α) reaction product were strikingly different from the values predicted by this mechanism. Whereas the theoretical ranges increased with bombarding energy in the expected manner, the measured values showed a more complicated behavior. Between 12 and 15 MeV the ranges increased with energy but were some 50% smaller than the calculated values. At this point the ranges began to decrease sharply with increasing bombarding energy, becoming about a factor of 2 smaller than expected for compound-nucleus formation in the neighborhood of 24 MeV. The ranges once again increased with incident energy above 27 MeV but remained nearly a factor of 3 smaller than predicted at 32 MeV, the highest energy investigated.

This unusual energy dependence suggests that various processes may be contributing to the (He^3,α) reaction. A direct pickup process undoubtedly is of importance at all energies. The angular distribution of α particles emitted in (He^3,α) reactions has been measured for a number of targets in the mass and energy region of present interest.[3–7] The differential cross sections of α groups leading to the ground state or low-lying excited levels of the product were usually found to be in good agreement with distorted-wave (DW) calculations. On the other hand, the low-energy α particles, which populate the highly excited states of the product, were more characteristic of an evaporation process. Also, other reaction paths are significant in measurements on residual nuclei. For instance, the emission of two protons and two neutrons may become of importance at the higher energies.

In order to obtain more detailed information about the reaction in question, the angular distribution of the Cu^{64} product has been measured over the bombarding energy range 12–32 MeV. The experiments are described in Sec. II and the results are presented in Sec. III. In Sec. IV the reaction mechanism is investigated by comparison of the results with DW and statistical-theory calculations.

II. EXPERIMENTAL

The irradiations were performed with the external beam of the Argonne National Laboratory 60-in. cyclotron. A schematic diagram of the irradiation chamber is shown in Fig. 1. The beam was defined by two $\frac{1}{8}$-in. collimators located approximately 11 cm from the target. Degrader foils were placed on the upstream side of the first collimator. The target was located at the center of a circle defined by the catcher foil holder and was oriented at 45° to the beam. The holder had sufficiently large apertures at 0° and 180° to the beam to allow the latter to traverse the chamber with only minimal scattering. The chamber was evacuated by opening it to the cyclotron vacuum.

* Supported by the U. S. Atomic Energy Commission.
† Present address; Institute of Engineering Research, Kyoto University, Kyoto, Japan.
[1] G. B. Saha and N. T. Porile, Phys. Rev. **149**, 880 (1966).
[2] G. B. Saha and N. T. Porile, Phys. Rev. **151**, 907 (1966).
[3] A. G. Blair and H. E. Wegner, Phys. Rev. **127**, 1233 (1962).
[4] M. K. Brussel, D. E. Rundquist, and A. I. Yavin, Phys. Rev. **140**, B838 (1965).
[5] C. M. Fou and R. W. Zurmühle, Phys. Rev. **140**, B1283 (1965).
[6] C. M. Fou, R. W. Zurmühle, and L. W. Swenson, Phys. Rev. **144**, 927 (1966).
[7] L. L. Lee, Jr., C. Mayer-Böricke, and R. H. Siemssen, Phys. Rev. **147**, 797 (1966).

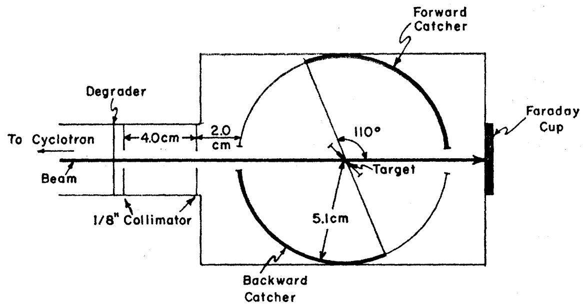

FIG. 1. Schematic diagram of irradiation chamber.

The target foil consisted of 0.0005-in.-thick silver having a nominal purity of 99.999%. Highly enriched[8] (99.7%) Cu^{65} was electrodeposited on both sides of this foil to a thickness of 8–12 $\mu g/cm^2$. The copper on the side of the foil, oriented at 45° to the beam, served as the source of forward recoils while that on the other side of the silver foil was used to produce recoils emitted in the backward direction. The silver foil was sufficiently thick to stop those recoils directed into the foil.

The catcher foil holder was of cylindrical shape and had a radius of 5.1 cm. The target was rigidly located at the center of the cylinder. The catcher foil consisted of 0.0008-in.-thick aluminum having a purity of 99.999%. Following the irradiations at 32.2 and 27.6 MeV, a 0.9-cm-wide strip was cut from the center of the collection foil for analysis. This strip was cut into 0.9×0.9-cm^2 pieces, each of which correspond to an angular interval of 10°. All these squares subtended practically equal (within 1%) solid angles. In the case of the bombardments at 22.1, 16.7, and 12.1 MeV, a 1.8-cm-wide aluminum strip was used for the angular-distribution measurements. The strip was cut into arc-shaped segments, concentric with the 0° or 180° positions and 1.8-cm wide in the middle. These segments covered angular intervals of 20°.[9] Small solid-angle corrections (<10%) were applied on the basis of the area of each segment.

The portion of the catcher foil that viewed the forwardly oriented target was used to determine the angular distribution between 0° and 110° while that facing the oppositely oriented target provided the data over the interval from 70°–170°. The forward and backward distributions thus overlapped between 70° and 110°. The disintegration rates of the overlapping samples were used to normalize the two distributions to each other. The need for normalization arose from the difference in the thickness of the two targets and from the energy degradation of the beam in the silver backing foil. At the lowest bombarding energy the degradation in the target backing was 2 MeV, which, because of the steep excitation function for the reaction,[2] led to substantially differing numbers of recoils originating from the two targets.[10] The energy resolution of the incident beam was sufficiently poor so that no substantial change in the angular distribution between the energies corresponding to the forward and backward targets was anticipated. The results are thus given for the average value of the bombarding energy.

Prior to irradiation the target assembly was carefully lined up with respect to the beam to ensure that the latter passed through the center of the target as well as through the apertures in the catcher assembly. This was accomplished by placing Mylar foils in the appropriate holder positions and determining the position of the beam spot following an irradiation of a few seconds.

The irradiations had a duration of 3–4 h and the beam intensity was kept at approximately 1μA. The energy of the incident beam was determined with a range-energy relation based on that of Bichsel *et al.*[11] for protons.

The possibility that Cu^{64} could be produced directly in the aluminum or from reactions originating in the silver backing foil was checked in an activation experiment. It was found that the over-all contribution from these sources was completely negligible, even at angles close to 0° or 180°.

After irradiation the collector strips were cut in the manner described above and copper was radiochemically separated from each foil.[1,12] The radioactivity of Cu^{64} was assayed with β proportional counters having a background of 0.5 counts/min. An empirically determined self-absorption curve was used to make small corrections for differences in sample thickness. The chemical yields of the various samples were determined gravimetrically. The decay curves were analyzed by means of the CLSQ computer program.[13]

III. RESULTS

The angular-distribution data are summarized in Table I. For each experiment the table lists the beam energy and target thickness corresponding, respectively, to the measurements at forward and backward angles as well as the average incident energy. The disintegration rates were converted to differential cross sections in the manner outlined in Sec. II, and the latter are given in arbitrary units in the table.

In addition to the uncertainties associated with the activity measurements and to several other minor random errors, the results are subject to the uncertainty introduced by the normalization between the forward and backward samples. The standard deviations of the average normalization factors obtained from the various overlapping samples are listed in Table I as a percent-

[8] Obtained from Oak Ridge National Laboratory.
[9] An 0.9-cm-wide segment, corresponding to the 0°–10° interval, was also cut from the strip.

[10] The data at 32 MeV were obtained in two separate irradiations. These results required no normalization for energy differences.
[11] H. Bichsel, R. Mozley, and W. Aron, Phys. Rev. **105**, 1788 (1957).
[12] N. T. Porile and D. L. Morrison, Phys. Rev. **116**, 1193 (1959).
[13] J. B. Cumming, U. S. Atomic Energy Commission Report No. NAS-NS3107, 1962, p. 25 (unpublished).

TABLE I. Angular distribution data.

θ_{min} (deg)	θ_{max} (deg)	$\langle\theta\rangle$ (deg)	Disintegration rate (d/min) Forward direction 32.2 MeV[a] (9.0 μg/cm²)[b]	Disintegration rate (d/min) Backward direction 32.2 MeV[a] (9.0 μg/cm²)[b]	$(d\sigma/d\Omega)$ arbitrary units 32.2 MeV[c]
0	10	5			
10	20	15	678 ±17		0.29[d]
20	30	25	335 ±11		0.14
30	40	35	201 ±12		0.087
40	50	45	121 ± 7.9		0.052
50	60	55	85.2± 4.2		0.037
60	70	65	52.8± 2.9		0.023
70	80	75	74.2± 7.2	48.0± 3.8	0.034
80	90	85		42.6± 8.7	0.030
90	100	95	77.3± 6.6	42.8±11	0.031
100	110	105	62.4± 4.3	57.5± 8.3	0.033
110	120	115		57.7±10	0.039
120	130	125		73.6± 3.1	0.050
130	140	135		70.5± 7.9	0.048
140	150	145		68 ± 3.5	0.046
150	160	155		59.1±11	0.040
160	170	165		74.5± 4.1	0.050
170	180	175			
			27.0 MeV (8.0 μg/cm²)	28.1 MeV (10.5 μg/cm²)	27.6 MeV
0	10	5	141 ± 7.8	...	0.015[e]
10	20	15	82.7± 3.9		0.087
20	30	25	78.7± 4.1		0.083
30	40	35	68.7± 2.9		0.072
40	50	45	50.9± 1.8		0.054
50	60	55	53.4± 1.2		0.035
60	70	65	21.2± 1.4		0.022
70	80	75	27.3± 1.7	16.6± 0.9	0.024
80	90	85	40.8± 1.8	43.9± 3.2	0.047
90	100	95	46.6± 1.2	40.3± 1.4	0.046
100	110	105	48.2± 2.1	47.7± 1.6	0.053
110	120	115		51.7± 1.8	0.060
120	130	125		49.3± 1.3	0.057
130	140	135		42.8± 1.5	0.049
140	150	145		44.6± 1.5	0.052
150	160	155		51.1± 1.7	0.059
160	170	165		45.8± 1.2	0.053
170	180	175			
			21.4 MeV (12.0 μg/cm²)	22.8 MeV (11.0 μg/cm²)	22.1 MeV
0	10	5	293 ± 4.6		0.15[f]
10	30	20	311 ± 4 9		0.11
30	50	40	198 ± 3.7		0.077
50	70	60	171 ± 3.2		0.067
70	90	80	307 ± 2.2	279± 2.9	0.11
90	110	100	333 ± 2.6	252± 3.4	0.14
110	130	120		317± 3.1	0.13
130	150	140		351± 3.2	0.10
150	170	160		241± 2.3	0.11
			16.1 MeV (12.0 μg/cm²)	17.3 MeV (10.0 μg/cm²)	16.7 MeV
0	10	5	85.1± 1.9		0.17[g]
10	30	20	68.8± 1.2		0.14
30	50	40	64.8± 1.6		0.13
50	70	60	67.6± 1.3		0.13
70	90	80	70.8± 0.5	54.5± 0.7	0.12
90	110	100	41.1± 0.8	71.7± 1.4	0.10
110	130	120		48.9± 0.8	0.085
130	150	140		43.5± 1.1	0.076
150	170	160		31.2± 5.0	0.054

TABLE I. (*continued*).

θ_{min} (deg)	θ_{max} (deg)	$\langle\theta\rangle$ (deg)	Disintegration rate (d/min) Forward direction 11.1 MeV (11.5 μg/cm²)	Disintegration rate (d/min) Backward direction 13.1 MeV (12.0 μg/cm²)	($d\sigma/d\Omega$) 12.1 MeV
0	10	5	41.8± 1.1		0.21[h]
10	30	20	52.7± 2.1		0.19
30	50	40	46.0± 1.3		0.18
50	70	60	43.6± 1.8		0.17
70	90	80	30.2± 2.0	78 ± 1.8	0.11
90	110	100	12.3± 0.6	52 ± 1.8	0.057
110	130	120		33.8± 1.9	0.043
130	150	140		19.1± 1.1	0.024
150	170	160		18.4± 1.0	0.022

[a] Bombarding energy.
[b] Target thickness.
[c] Average bombarding energy.
[d] Normalization error =14%. Statistical uncertainty in normalization factor =13%.
[e] Normalization error =14%. Statistical uncertainty in normalization factor =6%.
[f] Normalization error =9%. Statistical uncertainty in normalization factor =1%.
[g] Normalization error =39%. Statistical uncertainty in normalization factor =4%.
[h] Normalization error =24%. Statistical uncertainty in normalization factor =22%.

age error. These uncertainties are seen to range from 9–39%. These uncertainties are in part due to the statistical uncertainties of the activity measurements. The average percentage errors of the normalization factors due to this source are also summarized in Table I. It is seen that at 12 and 32 MeV the statistical uncertainty accounts for practically the entire normalization error, whereas at the other bombarding energies it is of smaller significance. The scattering of recoils in the target is another possible source of error. We believe, however, that this process has a negligible effect on the results. This belief is based on a recent[14] determination of the effect of target thickness on the angular distribution of (He^3, xn) reaction products from copper. It was found that the angular distribution was independent of thickness for targets of comparable thickness to the present ones.

The differential cross sections are plotted in Fig. 2. In those instances where the uncertainties are larger than the sizes of the points, representative error bars are shown. It is seen that the curves are very broad and do not exhibit the sharp dropoff with increasing angle found[15] in the case of the (α, xn) or ($\alpha, \alpha n$) reactions of Cu^{65}. At the lowest energies the curves are rather featureless. As the bombarding energy increases, it is seen that a minimum develops in the neighborhood of 60°. At the highest energy this minimum is also accompanied by a pronounced peak at forward angles.

IV. COMPARISON WITH CALCULATION

A. Direct-Interaction Calculation

The interpretation of the angular-distribution data is facilitated by comparison with various theoretical models of the reaction mechanism. The most likely mechanism for a (He^3,α) reaction involves the pickup of a target neutron by the incident He^3. In particular, the (DW) theory of direct reactions has been successfully used to fit the angular distributions of α particles emitted in (He^3,α) reactions.[3–7] We have consequently performed a DW calculation of the angular distribution of Cu^{64} nuclei produced in the (He^3,α) reaction. A similar calculation of the angular distribution of C^{11} recoils resulting from the C^{12}(He^3,α) reaction has been reported recently.[16]

The calculation of the differential cross section for the emitted α particle in the c.m. system, $d\sigma(\theta)/d\Omega$, was performed with the code JULIE.[17] In DW theory this

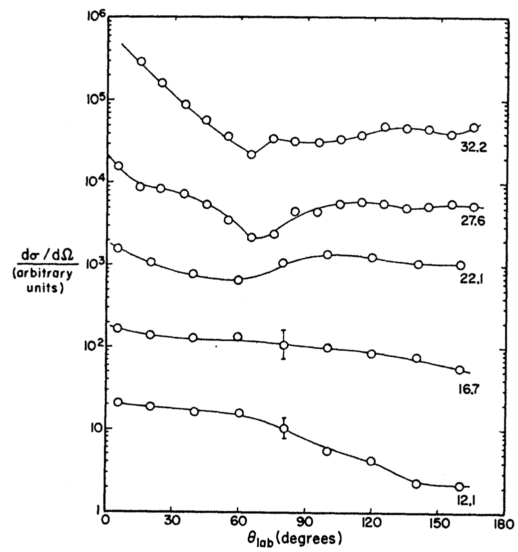

FIG. 2. Differential cross sections for the formation of Cu^{64}. The units are arbitrary and the curves are displaced from each other. The bombarding energy is indicated below each curve.

[14] I. Fujiwara and N. T. Porile, Phys. Rev. (to be published).
[15] N. T. Porile and G. B. Saha, Phys. Rev. 158, 1027 (1967).
[16] R. L. Hahn, Nucl. Phys. A101, 545 (1967).
[17] R. H. Bassel, R. M. Drisko, and G. R. Satchler, Oak Ridge National Laboratory Report No. ORNL-3240, 1962 (unpublished).

TABLE II. Optical-model parameters for entrance and exit channels.[a]

Reaction channel	V (MeV)	W (MeV)	r_0 (F)	r_c (F)	r_w (F)	a (F)	a_w (F)
Entrance[b] (He^3+Ni^{58})	180	35.0	1.06	1.40	1.50	0.733	0.835
Exit[b] (He^4+Ni^{58}, Fe^{56})	134.3	10.9	1.466	1.40	1.466	0.517	0.517

[a] The parameters are defined in Ref. 17. The computation used a radius cutoff of 5 F.
[b] The data are from Ref. 5.

quantity is related to the reduced cross section $\sigma_{lj}(\theta)$ for the transferred nucleon with orbital angular momentum l and total angular momentum j by the relation

$$d\sigma(\theta)/d\Omega=\tfrac{1}{2}NS_{lj}\sigma_{lj}(\theta)\,, \qquad (1)$$

where N is a factor that includes the strength of the nuclear interaction and the overlap between He^3+n and α, the particles involved in the nucleon transfer, and S_{lj} is the spectroscopic factor.

In the DW computation, the interaction is described in terms of DW's for the entrance and exit channels and of the bound-state wave function of the transferred nucleon. The latter was generated using a Woods-Saxon potential with potential-well radius of 1.25 F, charge radius of 1 F, and diffuseness parameter of 0.65 F. Also, the well depth was adjusted to fit the observed binding energy of the transferred neutron in Cu^{65}.

The optical-model parameters for the entrance and exit channels were obtained from published data on elastic scattering.[5] The entrance-channel values were based on the elastic scattering of 18-MeV He^3 from Ni^{58}; the exit-channel values were based on that of 21-MeV He^4 from Ni^{58} and Fe^{56}. The parameters are summarized in Table II.

In order to make the most meaningful comparisons with the experimental data is is necessary to compute the differential cross sections for the emission of α particles to both the ground and the various excited states of Cu^{64}. We have been unable to do this because of the lack of information on the spin-parities and spectroscopic factors of the excited states of Cu^{64}. The calculation has thus only been performed for the formation of Cu^{64} in its ground state following the pickup of a neutron from the $1f_{5/2}$ shell. This transition requires $l=3$. In order to test the sensitivity of the results to the assumed l value, we have also computed the differential cross section for an $l=1$ transition associated with the pickup of a $2p_{3/2}$ neutron.

The values of $d\sigma(\theta)/d\Omega$ obtained by use of JULIE for the α particle were first converted to the corresponding differential cross sections of Cu^{64} in the c.m. system. In view of the fact that the final state of the reaction involves only two particles, i.e., Cu^{64} and α, this transformation merely involved a change in angle from θ to $\pi-\theta$. The calculated values were subsequently trans-

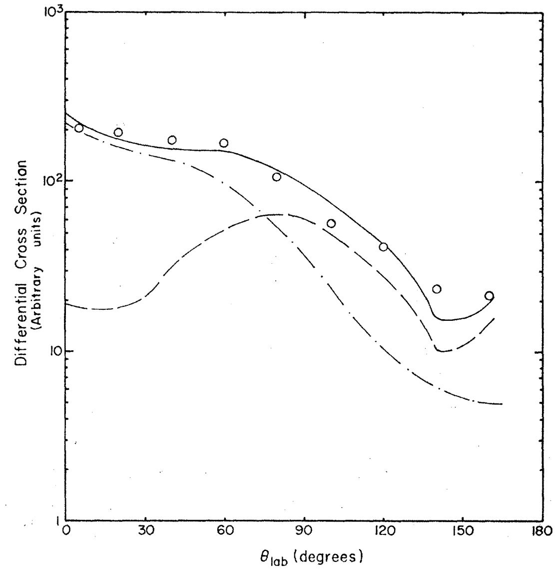

FIG. 3. Comparison of calculated and experimental differential cross sections at 12.1 MeV. Dashed line, DW calculation; dot-dashed line, statistical calculation; solid line, sum curve. The DW and statistical calculations have been adjusted in relative magnitude so that their sum gives the best fit to the experimental points.

formed[18] to the laboratory system for comparison with experiment. The laboratory recoil angle θ_{lab} is related to the c.m. recoil angle θ_R by the expression

$$\tan\theta_{lab}=(\sin\theta_R)/(X+\cos\theta_R)\,. \qquad (2)$$

The transformation parameter X is defined as

$$X=\left[\frac{A_b}{A_p}\frac{A_R}{A_T}\left(1+\frac{A_T+A_b}{A_T}\frac{Q}{E_b}\right)^{-1}\right]^{1/2}, \qquad (3)$$

where A_b, A_R, A_p, and A_T are the masses of the incident particle, recoil product, emitted particle, and target, respectively, E_b is the energy of the incident particle, and Q is the energy release of the reaction of interest. The differential cross section in the c.m. system $\sigma(\theta_R)$ transforms to that in the laboratory system $D(\theta_{lab})$ by the relation[15]

$$D(\theta_{lab})=\sigma(\theta_R)\frac{(X^2+2X\cos\theta_R+1)^{3/2}}{(1+X\cos\theta_R)}. \qquad (4)$$

The values of $d\sigma(\theta)/d\Omega$ were obtained from JULIE at angular intervals of 2.5°. The transformation in turn led to laboratory intervals of about 2°–7°. Since the experiments were performed with a 10° or 20° resolution, the calculated values were averaged over the experimental intervals. The distribution over an interval subtended by angles θ_1 and θ_2 was obtained from

[18] J. B. Marion, T. I. Arnette, and H. C. Owens, Oak Ridge National Laboratory Report No. ORNL-2574, 1959 (unpublished).

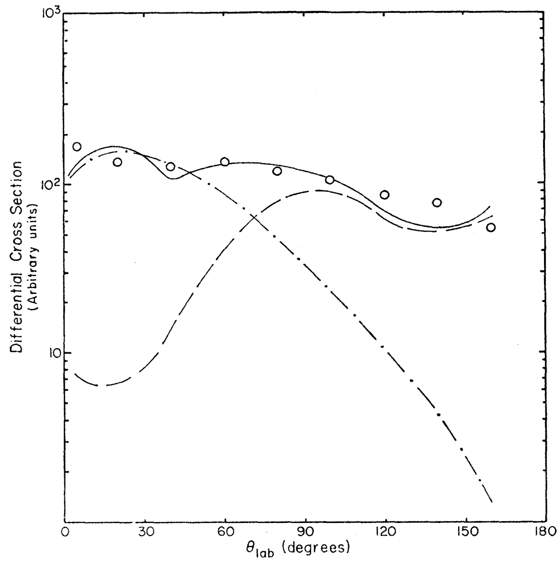

FIG. 4. Comparison of calculated and experimental differential cross sections at 16.7 MeV. See Fig. 3 for details.

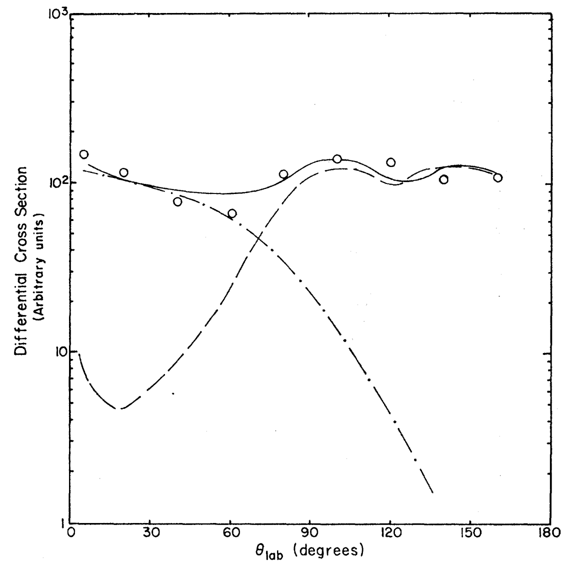

FIG. 5. Comparison of calculated and experimental differential cross sections at 22.5 MeV. See Fig. 3 for details.

the expression

$$\bar{D}\bar{\theta}_{12}=\int_{\theta_1}^{\theta_2} D(\theta)\sin\theta\, d\theta/(\cos\theta_1-\cos\theta_2)\,. \qquad (5)$$

The transformations were performed with a program written for the Purdue 7094 computer. The averaging procedure was done by numerical integration. The comparison with experiment is shown in Figs. 3–7. The calculated values are shown as a smooth curve drawn through the midpoints of the experimental intervals. The magnitude of the calculated differential cross sections was adjusted arbitrarily and only the comparison of the shapes of the curves is of significance.

The calculated curves exhibit a broad peak which moves from approximately 80° at the lowest energy to 180° at the top energy studied. This peak is a consequence of the predicted forward peaking of the α particles in the c.m. system. However, most of the structure present in the original calculation has been smoothed out by the averaging procedure. It is seen that while the calculated curves are rather similar in shape to the experimental ones at large angles, they are in complete disagreement at small angles. If the curves are thus normalized to each other at 160°, the calculated values at 0° are too small by one to two orders of magnitude.

In order to determine the sensitivity of the DW results to the assumed orbital angular momentum transfer and to the optical-model parameters, additional calculations were performed. Figure 8 shows the results of several DW calculations for an incident energy of 32 MeV. In addition to the previously discussed calculation, the figure includes curves based on the optical parameters summarized by Hodgson[19] for both $l=3$ and $l=1$. Although there are substantial differences between the various curves, none of them is able to account for the experimentally observed forward peaking. This conclusion holds true at lower bombarding energies as well.

B. Statistical-Theory Calculation

In view of the failure of the distorted-wave calculation to account for the observed angular distributions,

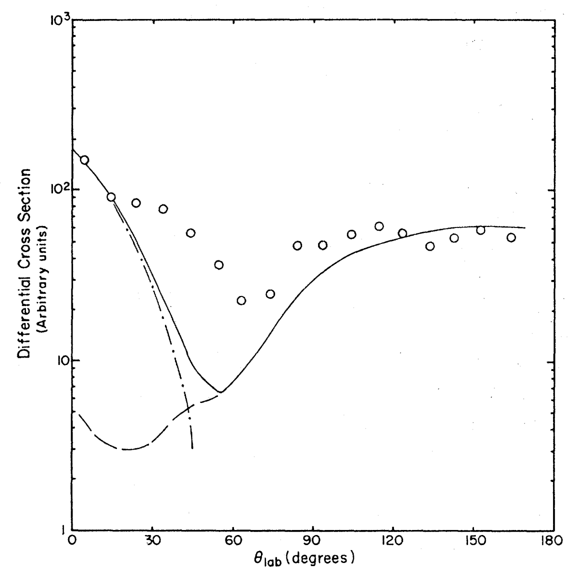

FIG. 6. Comparison of calculated and experimental differential cross sections at 27.6 MeV. See Fig. 3 for details.

[19] P. E. Hodgson, *The Optical Model of Elastic Scattering* (Oxford University Press, New York, 1963).

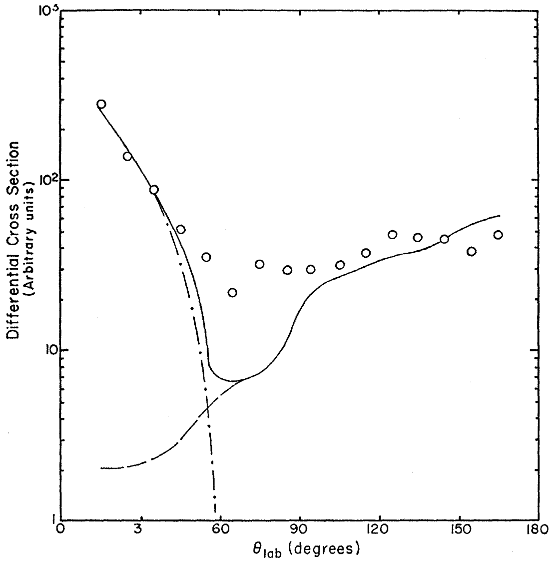

FIG. 7. Comparison of calculated and experimental differential cross sections at 32.2 MeV. See Fig. 3 for details.

a statistical-theory calculation was performed in order to investigate the importance of compound-nucleus formation. The calculation, which is based on the Monte Carlo code of Dostrovsky *et al.*,[20] has been described in detail in a previous paper.[15]

Since the calculated cross section for producing Cu^{64} by evaporation of an α particle is known to be small,[2] the program was modified to reduce the amonut of computer time required to produce adequate statistics. The calculation for comparison with the 12–22 MeV data required that the first particle emitted from the compound nucleus be an α particle. Thereafter, the residual nucleus was free to emit nucleons as well as α particles. This modification does not introduce any bias in a spin-independent analysis such as the present one. It was found that the calculation was speeded up by a factor of 10–100, depending on the bombarding energy. Enough iterations were performed to yield a minimum of 2000 Cu^{64} events.

At incident energies above 22 MeV the probability for producing Cu^{64} by means of α-particle evaporation becomes vanishingly small. The only significant contribution to the calculated cross section is from the emission of four nucleons. The calculation at the higher energies was accordingly programmed to include only neutron and proton emission. The results for comparison with the 32-MeV data are based on 500 events. The predicted cross section at 27 MeV was too small to lead to a meaningfully large number of events and the calculated curve is not well defined.

The results of the calculation are shown in Figs. 3–7. It is seen that in the energy range where α-particle

[20] I. Dostrovsky, Z. Fraenkel, and G. Friedlander, Phys. Rev. **116**, 683 (1959).

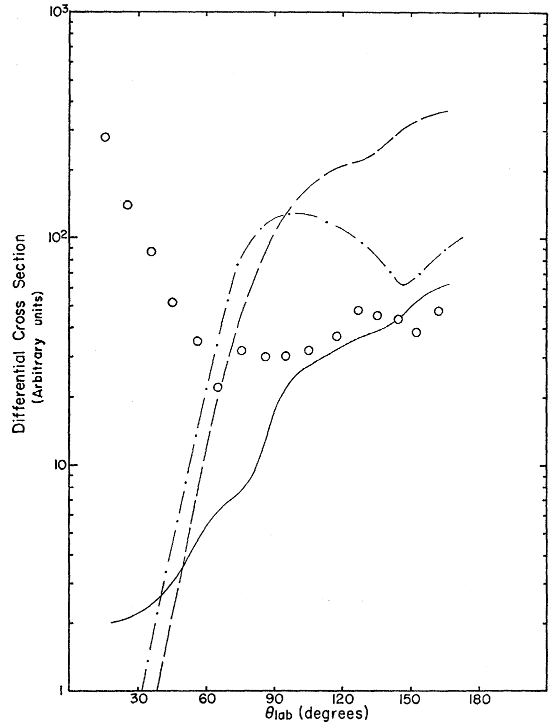

FIG. 8. Dependence of DW calculation at 32.2 MeV on various parameters. Solid curve, previously described differential cross section; dashed curve, based on optical parameters from Ref. 19 and $l=3$; dot-dashed curve, based on optical parameters from Ref. 19 and $l=1$. The experimental points are shown for comparison.

emission leads to the reaction product the calculated curves are very broad and extend into the backward direction. This is due to the fact that the more energetic α particles have a larger momentum than the incident He^3 does. The emission of an α particle in the forward direction will under these circumstances lead to backward recoil. By contrast, the evaporation of four nucleons leads to a much narrower angular distribution.

The calculated and experimental curves are seen to markedly differ in shape from each other at all energies. The disagreement is particularly noticeable at large angles, especially at the higher energies. This result is not surprising in view of the difference between the average projected ranges[2] of Cu^{64} and the compound-nuclear values.

V. CONCLUSIONS

The comparison of the angular-distribution results with calculated values based on either the DW or the statistical theory indicate that neither model can adequately account for the results. It is apparent, however, that a combination of the two calculated curves can give a reasonably good fit to the data. We have adjusted the magnitudes of the calculated curves in such a fashion as to produce the best over-all fit with experiment, as determined by a χ^2 test.

The comparison of the synthetic curves with experiment is given in Figs. 3–7. The compound-nuclear mechanism contributes principally to the differential cross sections at forward angles, especially at the higher energies where nucleon evaporation is of importance. On the other hand, the direct process accounts primarily for the yield at large angles. It is seen that the calculated curves are now in rather good agreement with the data except for the region of 40°–100° at the higher energies where a substantial discrepancy remains.

The adjustment of the two calculated sets of curves indicates that the compound-nuclear process accounts for some 40–70% of the reaction cross section, depending on the bombarding energy. This estimate undoubtedly represents an upper limit because the contributions from pickup processes leading to excited states of Cu^{64} would result in a fit involving a larger percentage of direct interaction. The average range measurements suggest, in fact, that pickup must account for well over half the reaction cross section. Our angular-distribution results are qualitatively consistent with this finding.

ACKNOWLEDGMENTS

We would like to acknowledge the cooperation of M. Oselka and the operating crew of the Argonne cyclotron. Thanks are due to Dr. R. Drisko for valuable discussions.

PHYSICAL REVIEW VOLUME 170, NUMBER 4 20 JUNE 1968

Pairing-Model Calculation of Nuclear Matrix Elements in the Decay of ^{74}As

H. Ogata and E. E. Habib
Department of Physics, University of Windsor, Windsor, Ontario, Canada

(Received 13 November 1967)

The matrix elements $C_A\int\boldsymbol{\sigma}\cdot\mathbf{r}$, $C_A\int\mathbf{r}$, $C_V\int i\boldsymbol{\sigma}\times\mathbf{r}$, and $C_A\int B_{ij}$ are calculated for ^{74}As, using the pairing model. $C_V\int i\boldsymbol{\alpha}$ is determined from the conserved vector current theory, and $C_A\int i\gamma_5$ from β-γ angular correlation data. The ratio of the $(\int B_{ij})^1/(\int B_{ij})^2$ for the β transitions to the ground state and first excited state, respectively, of ^{74}Ge is calculated from these matrix elements and the β intensities. This ratio is also calculated solely from the model and compared with the above ratio to check the internal consistency of the method. The results show that better agreement is obtained if the effect of phonon-quasiparticle coupling is included.

I. INTRODUCTION

The first forbidden nonunique β decays are of special interest in determining nuclear structure. Unlike the unique transition for which the only nuclear matrix element involved is the B_{ij} term, the nonunique transitions require, in general, all six nuclear matrix elements to be considered. One of the indications of this fact is the small A_2 coefficients with a positive sign often observed in the β-γ angular correlation, which should be negative and one order of magnitude larger if the j selection rule is strictly satisfied. Another indication is that the B_{ij} ratio deduced from the β intensities to the ground state and first excited state disagrees with the estimated ratio significantly. These facts suggest that the nonvanishing lower-rank nuclear matrix elements can give information about nuclear structure, since they should vanish if we apply the ordinary shell model. Finite values of these matrix elements indicate departure from the simple shell-model configurations.

In this connection, Matsumoto *et al.* examined different models, but none of them successfully explained the observed data.[1] Recently, calculations based on the pairing model were made,[2,3] but the agreement of these calculations with the experimental data was not very good. We have made similar calculations, and the results indicate that the coupling between the quasiparticle and the phonon states is very important.

In the following sections we first review shell-model considerations and then explain the model we have used. Numerical results for the decay of ^{74}As to the first excited 2^+ state of ^{74}Ge are given, and a summary and discussion are presented in the last section.

II. SHELL-MODEL CONSIDERATION OF THE POSITRON DECAY OF ^{74}As

According to the shell model, the net process for the decay of ^{74}As is a transition of a proton in the $(\pi f_{5/2})$ shell to a neutron in the $(\nu g_{9/2})$ shell. This implies that the spin change $\Delta j=2$ with a parity change is the only possible transition because of the shell-model j-selection rule. On the other hand, the experimental results show that this is not the only possibility, but there must be interactions due to lower-rank tensors as well as the dominant one due to the highest-rank tensor.[4]

[1] Z. Matsumoto, M. Yamada, I. T. Wang, and M. Morita, Phys. Rev. **129**, 1308 (1963).

[2] L. S. Kisslinger and Chi-Shiang Wu, Phys. Rev. **136**, B1254 (1964).

[3] S. Wahlborn, Nucl. Phys. **58**, 209 (1964).

[4] E. E. Habib, H. Ogata, and W. Armstrong, Can. J. Phys. **44**, 1157 (1966).